Novel Mechanisms for Defect Formation and Surface Molecular Processes in Virus Crystallization

A. J. Malkin* and A. McPherson

Department of Molecular Biology and Biochemistry, University of California, Irvine, 560 Steinhaus Hall, Irvine, California 92697-3900

Received: December 18, 2001

The in situ atomic force microscopy (AFM) investigation reveals the sources of disorder in crystals of an icosahedral plant virus, cucumber mosaic virus (CMV). It is here demonstrated that CMV virions that form a new 2D nuclei on (001) faces bind in arbitrary positions. This results in the formation of new growth layers with height differences in the range 0.5−2 nm. Coalescence of growth layers with height differences of up to 2 nm proceed without defect formation, while the merger of those with greater differences in height proceed with formation of domain boundaries. As a result, the (001) faces of hexagonal CMV crystals are formed by numerous misoriented domains with sizes in the range 0.5−50 μm^2. A variety of abnormal virions that have diverse sizes and that frequently cause defect formation were visualized in the CMV crystalline lattice. The combination of defects and local disorder presented here are likely the physical bases for mosaicity in crystals and may be largely responsible for their limited diffraction resolution. Studies of molecular mobility on the virus crystalline surface revealed the initial stages of two-dimensional nucleation as well as the mechanisms for virion incorporation into the step edges. The molecular structures of the step edges, which advance by the mechanism of one-dimensional (1D) nucleation, were recorded, and attachment rates of individual virions into growth steps were measured. From these data, the attachment frequencies were measured and the attachment probability for CMV crystallization was estimated to be approximately 10^{-2}.

1. Introduction

High-resolution structures of macromolecules obtained from X-ray crystallographic analyses are necessary to provide the architectural basis for a comprehensive understanding of biological systems and processes at the molecular level. This foundation is critical, for example, in correlating structures and functions of proteins emerging from structural genomics, and it is an essential tool for further development of rational drug design, protein engineering, and pharmaceutical formulation of protein drugs. The precision of structural information derived from X-ray crystallography is ultimately limited by the imperfections and disorder that characterize macromolecular crystals.

Currently, a limited understanding of the mechanisms operative in crystallization, and their impact on the solid-state properties of macromolecular crystals, restrict a broader application of X-ray diffraction analysis in biotechnology. Studies of the defect structures of macromolecular crystals by different techniques has revealed the presence of a wide variety of defects, including incorporated impurity macromolecules and microcrystals, point defects, inclusions, interstitials, dislocations, stacking faults, cracks, and twins.[1−5] Defect densities for several macromolecular crystals have also been estimated.[3] However, despite much recent progress in the physical analyses of macromolecular crystallization,[1−16] important questions remain largely unanswered, particularly, which kinds of disorder limit the diffraction resolution, and what are the sources of the disorder that arise during growth? Furthermore, studies on molecular dynamics on surfaces of macromolecular crystals, which are vital for the further development of a quantitative understanding of the crystal growth process and defect formation, were conducted for crystallization of only a few macromolecules.[5−7,10]

The crystallization of different families of icosahedral viruses having diameters in the range 17−30 nm provides a particularly useful model system for investigating questions regarding macromolecular crystal growth. The virions are virtually spherical, crystallize easily, and each particle is of such a size that it can be readily visualized by AFM. Because of these large particle sizes, height differences in the positions of virions in a surface layer as small as a few percent can be reliably detected by AFM. This is not the case for most of proteins, whose smaller sizes make it difficult or impossible. Growth is sufficiently slow that individual virus particles can be directly observed as they absorb onto a crystal surface or enter into its lattice. These features of spherical viruses, combined with the AFM technique, allow direct observation of events involving individual particles. Together they provide a powerful approach to the visualization of growth mechanisms and dynamic surface phenomena, and they yield new insights into the sources of crystal disorder and the formation of defect structure.

This approach, as is seen in the crystallization of cucumber mosaic virus (CMV), permits visualization of adsorption of individual virions and their complexes on the crystalline surface, initial stages of two-dimensional (2D) nucleation, and mechanisms of incorporation of virions into growth steps. Furthermore, formation of multiple misoriented domains upon merger of 2D nuclei usually resulted in a high degree of imperfection. It was demonstrated that due to the apparent weak binding between growth layers on the (001) face of CMV crystals, virions forming new 2D nuclei adsorb in the arbitrary positions on the surface. This results in the formation of nuclei, which are

* Corresponding author. Phone: (949) 824-4397. Fax: (949) 824-1954. E-mail: amalkin@uci.edu.

10.1021/jp014580d CCC: $22.00
Published on Web 06/11/2002

misoriented with respect to each other, with a height difference in the growth layer as large as 5 nm. Subsequent formation of multiple domains then occurs upon merger of 2D nuclei (section 3.1). This is the first report of such phenomena for any conventional and macromolecular systems, and it is significant because defects and disorder are the primary constraints in obtaining atomic resolution structure from macromolecular crystals. Mosaic structure of CMV crystals and incorporation of aberrant virions in the crystalline lattice (section 3.2) could explain the poor diffraction properties of CMV crystals (section 3.3). Quantitative measurements of incorporation of the virions into the growth steps allowed estimation of attachment frequencies and probabilities (section 3.4).

2. Experimental Section

The study we describe here used a $T = 3$ virus of 28 nm diameter, cucumber mosaic virus (CMV), whose capsid is composed of 180 identical protein subunits and whose genome is single stranded RNA.[17] CMV is the member of *Bromoviridae* family that infects over 800 plant species worldwide.[18] CMV was propagated in *Nicotiana tabacum* and purified using the protocol of Lot et al.[19,20] The virus forms crystals of cubic and hexagonal plate habit. The latter crystals are the subject of the work presented here. CMV crystals having a hexagonal plate shape were grown using the vapor diffusion method consisting of mixing 3−7 mg/mL CMV in H_2O with 1 M ammonium phosphate (pH = 7.6) and had sizes in the range 50−75 μm. From X-ray diffraction analysis using synchrotron radiation the crystals are of rhombohedral space group $R3$ with $a = b = c =$ 291.4 Å and $\gamma = 109°$ (equivalent hexagonal unit cell $a = b =$ 475.4 Å, $c = 299.2$ Å). The rhombohedral unit cell contains a single virion, and an icosahedral threefold axis is coincident with the unique crystallographic axis. The crystals generally diffract to no better than 10 Å resolution, and in the best of cases to about 4 Å.

Seed crystals were mounted on the plastic disk and then transferred into the AFM fluid cell, which was subsequently filled with a mixture of virus and precipitant solution. Images were collected in tapping mode using a Nanoscope IIIa AFM (Digital Instruments, Santa Barbara, CA) with Olympus oxide sharpened silicon nitride tips purchased from Digital Instruments. All operations were carried out under crystallization conditions, in a fluid-filled cell, with the supersaturation controlled by the virus concentration. The diffusion coefficient of CMV was determined using a Malvern 4700c submicro particle analyzer (Malvern Instruments, Inc., Southborough, MA).

3. Results and Discussion

3.1. Domain Structure of CMV Crystals and Mechanisms of Its Formation. AFM images of the (001) face of CMV crystals revealed numerous domains with sizes in the range 0.2−50 μm^2. Domain boundaries are clearly evident in Figure 1. In some cases the virion surface lattice within an individual domain is misoriented with respect to the virion lattice outside the domain, as shown in Figure 1b. The height difference between domains within the same surface growth layer varies from 0.6 nm to almost 5 nm, that is, by 2−18% of the diameter of the virus particles making up the lattice.

Layer growth on the (001) face of hexagonal crystals of CMV occurs by the progression of steps generated exclusively by two-dimensional nucleation (Figure 2). Step heights on the (001) face are not equal for different steps but vary in the range 25−30 nm, again approximately 18% of the particle diameter. Differences in step heights of this magnitude on the faces of

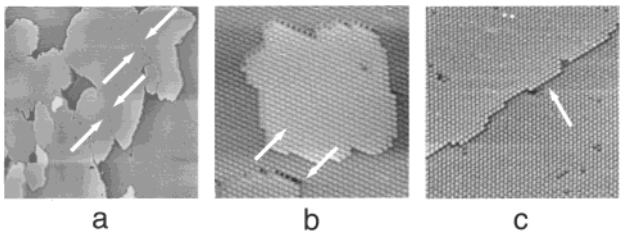

Figure 1. AFM images of the (001) face of CMV crystals showing in (a) large area revealing multiple domains (indicated with arrows). (b), (c) Higher magnification AFM images of domains (indicated with arrows). The scan areas are 18 × 18 μm^2 in (a), 1.3 × 1.3 μm^2 in (b), and 1.5 × 1.5 μm^2 in (c).

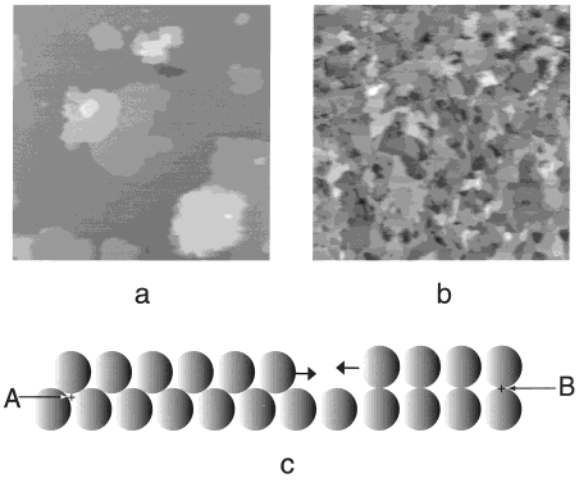

Figure 2. AFM images of the (001) face of CMV crystals showing 2D nucleation at relatively low (a) and high supersaturations (b). A cross section of the (001) face showing arbitrary attachment of virions on the underlying growth layer is in (c). AFM images are 16 × 16 μm^2 in (a) and 18 × 18 μm^2 in (b).

macromolecular crystals, or indeed any crystals, have not previously been observed. The smallest measured step heights of 25 nm correspond to precise alignment of growth steps upon the previous layer. Virions forming a new growth layer position themselves in triangular depressions formed by virions in the layer below, as shown in Figure 2c (position A). Steps having heights of 30 nm, on the other hand, have their constituent virions positioned atop particles in the preceding layer (position B in Figure 2c). CMV virions, it appears, form weak and geometrically imprecise bonds upon incorporation into crystals. The broad and continuous range of height differences among growth steps (0.5−5 nm) suggests that virions creating a new two-dimensional nucleus may attach arbitrarily at intermediate sites between positions A and B (Figure 2) on the preceding layer. Remarkably, even within a single domain a height difference between virions of up to 1.5 nm is observed. A two-dimensional nucleus, therefore, can grow by addition of virions that come to occupy significantly different crystallographic positions within the same growth layer.

Due to height variations, a significant number of individual two-dimensional nuclei are formed on the (001) face, which are crystallographically misoriented with respect to one another. Because of the nonrigorous nature of the molecular contacts in the lattice, coupled with an unusually high elasticity, growth layers with height differences of up to 2 nm may, nonetheless, merge without formation of defects. Examples are shown in Figure 3a−c. Coalescence of growth steps with larger height differences in the neighborhood of 3 nm and larger, seen in Figure 3d−f, results in formation of domain boundaries.

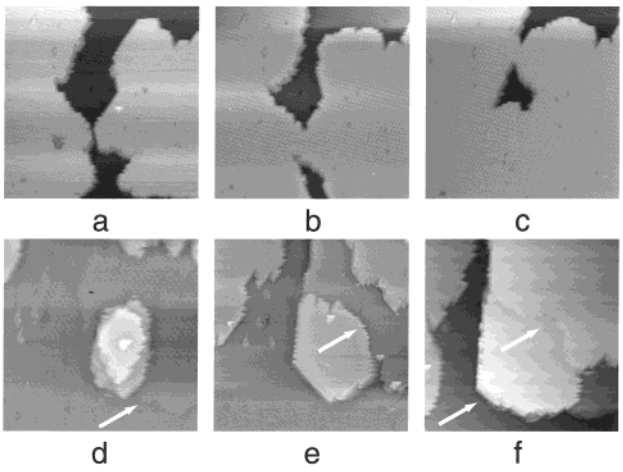

Figure 3. AFM images (a)−(c) showing the merger of growth steps without formation of defects. In (d) through (f) formation of domain boundaries arising from the merger of misoriented two-dimensional nuclei is seen. Preexisting and newly formed domain boundaries are indicated with arrows in (d)−(f). AFM images are $2 \times 2\ \mu m^2$ in (a)−(c), $2.75 \times 2.75\ \mu m^2$ in (d), $3.25 \times 3.25\ \mu m^2$ in (e), and $3 \times 3\ \mu m^2$ in (f).

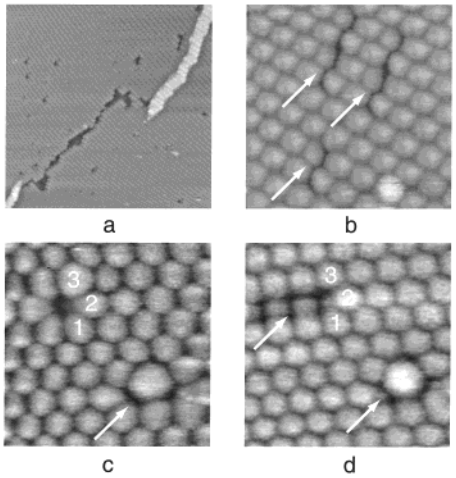

Figure 4. AFM images showing, in (a), two-dimensional nucleation within a fault on the (001) face of a CMV crystal. In (b) the incorporation of abnormal CMV virions with diameters in the range 22−26 nm (indicated with arrows) results in defect formation. In (c) the incorporation of two abnormally large virions into the crystalline lattice is seen. Anomalous particle incorporation can proceed either without defect formation, as in the example indicated by an arrow, or result in the formation of a point defect (where the aberrant particle is indicated by the number 3). In (d), the abnormally large virion indicated by the number 3 in (c), was displaced from the surface layer by the AFM tip. This was followed by a rearrangement of the surrounding virions in the crystalline lattice. AFM images are $3 \times 3\ \mu m^2$ in (a), $230 \times 230\ nm^2$ in (b), $190 \times 190\ nm^2$ in (c), and $210 \times 210\ nm^2$ in (d).

In Figure 3d, for example, a pair of two-dimensional nuclei appears in the proximity of a domain boundary. These nuclei merge in Figure 3e,f with additional growth steps arising from other two-dimensional nuclei. This results in a new boundary, which separates domains and has a height difference of approximately 4.6 nm (Figure 3f). Growth layers did not advance beyond the original domain boundary, seen in Figure 3d, which served as a barrier. Thus, such defects propagate throughout the volume of the crystal.

Growth by formation of misoriented 2D nuclei resulting in a domain structure has not been previously reported to our knowledge, either in crystallization of conventional or macromolecular crystals. Domain structures of different discommensurate phases have been observed for several metal/semiconductor systems,[21] and in gravity-sedimented colloid crystals.[22] While these two cases are superficially similar to the domain structure reported here, they are significantly different than those actually observed in CMV crystals. Formation of domains upon deposition of metal atoms on the surface of semiconductors is strictly a consequence of deviation in lattice mismatch. Following deposition of relatively small amounts of metal atoms, strain becomes sufficiently unfavorable that domains with sizes no greater than several hundred $Å^2$ form. Self-assembled colloidal crystals, while close-packed, are generally a polycrystalline mixture of randomly stacked crystals with face-centered-cubic (fcc) and hexagonal closed-packed (hcp) lattices. The extent of defects is a function of the assembly technique.[22] The source of mosaicity in CMV crystals, however, is the formation of growth steps of variable sizes due to the attachment of virions to arbitrary sites on the preceding layer during multiple two-dimensional nucleation under supersaturated conditions (Figure 2).

In addition to domain boundaries, the (001) face of hexagonal CMV crystals also contains deep faults such as those seen in Figure 4a. Their depth may vary from 10 to 14 nm. Such faults were seen in virtually all CMV crystals investigated. Because formation of the faults was not observed during in situ AFM imaging, the mechanisms by which they are created is not clear. Formation of misaligned domains as described above can, however, cause a significant accumulation of stress within a crystal and relaxation of this stress could produce the faults. In any case, under supersaturating conditions, two-dimensional nucleation was seen to take place in the wider regions of the faults. These nucleation sites then gave rise to layers, which extended 15−20 nm above the surrounding surface layer (Figure 4a). While distances between virions in these nascent domains are virtually the same as in the (001) plane, the local crystal lattice is clearly misoriented with respect to that of the surrounding growth layer.

3.2. Defect Formation Due to the Incorporation of Aberrant Virions and the Possibility of Defect Reconstruction with the AFM Tip. High-resolution AFM images of the surface layers of CMV crystals reveal the unexpected presence of abnormal virions with diameters in the range 22−36 nm, as exemplified by those seen in Figure 4b−d. In some cases incorporation of virions of abnormally large sizes do not result in the defect formation (Figure 4c), while in other cases incorporation of abnormal virions do cause defect formation seen in Figure 4b. In Figure 4b incorporation of abnormal virions causes local distortion, which propagates through several adjacent rows of virions and results in the defect formation. The density of these defects can be very high, up to $10^7\ cm^{-2}$, which is several orders of magnitude greater than point defect densities visualized for other macromolecular crystals.[3] CMV crystals tolerate the incorporation of aberrant virions having abnormal sizes, apparently without pronounced accumulation of lattice strain.

The presence of the aberrant particles from a strictly biological perspective is a unique and interesting observation in itself and likely reflects a high error rate in the assembly of virions in infected tissue, in this case, the cells of tobacco leaves. Attempts have been made using, for example, density gradient centrifugation to remove fractions of larger or smaller viruses. Nonetheless, despite these measures, the incorporation of aberrant particles into growing virus crystals was nonetheless observed.

Two classes of virus particles and their aggregates were observed on a crystalline surface. In the first case, upon

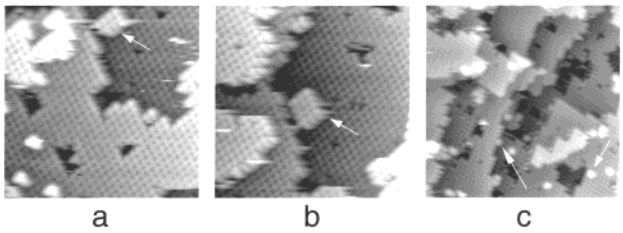

Figure 5. (a) and (b): Initial stages of development of supercritical 2D nuclei (indicated with arrows). (c) Incorporation of single virions into step edges and adsorption of single virions (one is indicated with a long arrow), on the crystalline surface. Also seen are virions (one is indicated with a short arrow) that remain firmly attached to the surface but do not develop into 2D nuclei. The scan areas are (a) 860 × 860 nm^2, (b) 1 × 1 μm^2, and (c) 1.4 × 1.4 μm^2.

adsorption, virus particles form small clusters. As expected, these develop into two-dimensional nuclei and provided sources of growth steps. In Figure 5a,b, for example, a 2D island consisting of approximately 9 virus particles expanded over 7 min by the addition of 3−4 virions. We also consistently observed virus particles having diameters of 28 nm and their clusters, which adsorb to the crystalline surface but never develop into two-dimensional nuclei (Figure 5c). This suggests that their interactions with the underlying surface are probably incompatible with the crystallographic lattice. These virus particles, however, appeared firmly attached to the surface and could be seen in subsequent images over long periods of time. Ultimately these virions and their clusters were incorporated in growth steps, often causing defect formation. Capsids of these virions have been modified during purification procedures. Alternatively, microheterogeneity of virions could arise from differing amounts of divalent cations bounded to virions. In either case, both aberrant and modified virions apparently form sufficient crystallographic interactions to be incorporated in the crystalline lattice.

AFM also proved effective in the molecular scale manipulation of defects in CMV crystals. For example, in the time between the AFM scans shown in Figure 4c,d, an anomalously large virion (indicated by the number 3 in Figure 4c) was displaced from the surface layer by applying an increased force with the AFM tip. This resulted in an immediate local rearrangement of virions in the crystalline lattice and disappearance of the point defect. This was accompanied by a further repositioning of two other virions (indicated with arrows). The dynamic behavior in response to physical perturbation illustrated here, for what otherwise might be taken as a static array of biochemical units, may have significant implications for self-assembly processes and their associated transitions.

3.3. Correlation between Observed Macro- and Microheterogeneities in CMV Crystals and Their Poor Diffraction Properties. Particle variability within the CMV lattice due to virion microheterogeneity results in poorer long-range order compared with other macromolecular crystals. In addition, weak intermolecular bonding produces hexagonal CMV crystals having extremely high mosaicity. Both of these sources of disorder are consistent with the poor diffraction properties of the crystals.

Macromolecular crystals, in general, exhibit considerably greater mosaic spread compared with conventional small-molecule crystals.[23,24] Crystals, including those of macromolecules and viruses, are traditionally described as consisting of misoriented mosaic blocks. Each mosaic block is, in turn, treated as a perfect crystal composed of molecules exhibiting varying degrees of local disorder.[24] In CMV crystals, blocks disrupted both long- and short-range lattice order, and the mechanisms by which they formed were evident. Mosaic block structure generally assumes that variation in domain orientation occurs on a length scale comparable to the crystal size. It arises from the domain structure of the crystalline faces, and those domains are, in turn, due to the coalescence of misoriented two-dimensional islands. Thus, the observations presented here are important in identifying the sources of mosaicity, which, to a great extent, determines the resolution limit and the ultimate quality of X-ray structure determinations. In the study presented here, the classical theory of mosaic blocks achieves physical reality.

Because of the arbitrary disposition of virions within individual domains and growth layers, their deviations from average lattice orientations and positions are considerable. This produces local disorder within the CMV crystals. Mosaicity and local disorder both affect diffraction properties. The local disorder we observe for CMV crystals is likely common in crystals of most viruses, and probably crystals of most macromolecules, and this could explain their generally poor diffraction properties.[23,24] Effects are simply accentuated in virus crystals because of the large particle size and unit cell dimensions.

CMV crystals diffract to little more than 10 Å resolution**.** This nonetheless suggests the presence of a significant degree of order. That is, within translationally disordered domains, most of virions are likely to be ordered in a manner consistent with crystallographic symmetry. Were the domains well ordered with respect to one another, then a well diffracting crystal would result. But, as we show here, in CMV, the domains suffer from translational displacements. It is this interdomain translational disorder that is probably responsible for the limitation of Bragg reflections to only 10 Å. It is quite likely that the disorder of most icosahedral virus crystals, which typically rarely diffract beyond 3.0 Å resolution[25−28] reflect the fundamental sources identified in this investigation, but generally to lesser degrees.

The diversity in particle size incorporation not only reflects the inherent microheterogeneity of the virion population, but it emphasizes the elasticity and remarkable degree of tolerance of the crystal lattice of virus crystals. It further suggests that the formation of domains and mosaic blocks ultimately arises from the natural statistical disorder and conformational variability of the macromolecules in the crystal lattice.

3.4. Incorporation of CMV Virions into CMV Crystals: Attachment Frequencies and Probabilities. Because of their relatively large sizes, CMV virions can be seen by AFM to incorporate into growth steps as individuals, thus allowing measurement of attachment frequencies under controlled supersaturation conditions. From attachment frequencies, attachment probabilities can be estimated.

In the case of inorganic crystals grown from solution, solvatation and desolvatation processes typically exhibit relatively high activation energies,[29] while the entropic activation barrier can be relatively low. The corresponding steric factor, which is the probability of a particle having the proper spatial orientation, is close to unity. In the crystallization of complex macromolecules, the necessity of desolvatation is likely less important than in the crystallization of inorganic molecules. However, macromolecules in an arbitrary orientation cannot join a growth site. Thus the entropic activation barrier must play an important role. Pre-kink selection would be expected for the approaching macromolecule to assume an acceptable orientation for incorporation into the growth step. In CMV crystals, icosahedral virions are connected in the surface layer through hexameric capsomers;[28] hence there are 60 identical orientations

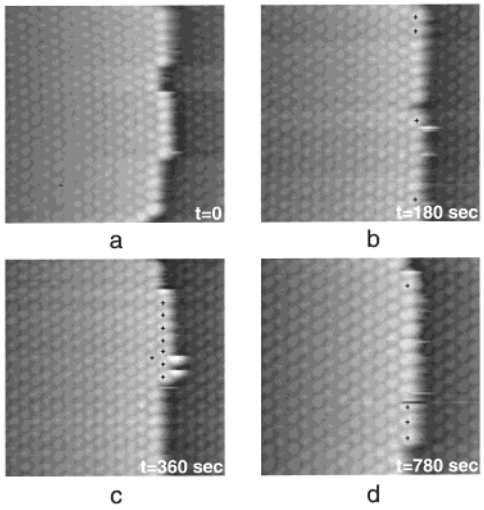

Figure 6. AFM images of an advancing growth step on the (001) face of a CMV crystal. Newly incorporated virions are indicated with +. AFM images are 670 × 670 nm^2 in (a)−(c) and 560 × 560 nm^2 in (d).

for correct incorporation, far more than for most proteins. This, given the weak and imprecise nature of bonding between virions in the (001) plane, incorporation should result in relatively high attachment probabilities.

As seen in Figure 6, advancement of growth steps proceeds by one-dimensional nucleation of kinks,[29] formed by single or multiple virions, with subsequent lateral extension of molecular rows by addition of virions into kinks. Similar mechanisms of step advancement have previously been described for other macromolecular crystals.[6,7,10,31] Under the supersaturation conditions here (∼0.1 mg/mL CMV), the attachment frequency of virus particles was found to be $\sim 2.3 \times 10^{-2}$ virions/s. There was no detachment of any virus particle, either at supersaturated or equilibrium conditions; hence, thermal energy is insufficient to displace a particle from the step edge.

In these experiments the concentration of virions in solution was $c = 7 \times 10^{12}$ cm^{-3}, corresponding to an average distance between virions of $L = 5 \times 10^{-5}$ cm. Assuming that growth proceeds by direct incorporation of virions from the bulk solution into the step edge[30] and that the concentration of virions at the crystalline interface is zero, then the diffusive flux can be estimated as $J = D(C - C_0)/L = 2.2 \times 10^{10}$ s^{-1} cm^{-2}. $D = 1.6 \times 10^{-7}$cm^2/s is the diffusivity of CMV determined from light scattering experiments. From this, virus particles encounter a kink having a size of approximately 30 × 30 nm with a frequency of approximately ∼0.2 s^{-1}. Using the attachment frequencies of 2.3×10^{-2} s^{-1} measured from AFM (Figure 6), the attachment probability is $\sim 10^{-2}$. Thus, approximately one out of every 100 CMV virions that approach the step edge incorporates into the step.

This probability of attachment can be related in large part to pre-kink selection of proper molecular orientation for incorporation into the growth step. For high symmetry particles, as might be expected, pre-kink selection of the proper molecular orientation is considerably less than for most macromolecules. Indeed, from the same calculation using AFM data for step advancement in thaumatin crystallization,[31] the attachment probability of those protein molecules, which can have only one correct molecular orientation for incorporation into the crystal, was estimated to be $\sim 5 \times 10^{-4}$. CMV particles crystallize with a high attachment probability because of their high symmetry and nonrigorous binding tendencies. These same properties undoubtedly explain as well the facile incorporation of large numbers of aberrant virions into the lattice, and the observed ability of growth layers to restructure as a consequence of physical perturbation.

Acknowledgment. We thank A. Greenwood, R. Lucas, and J. Zhou for technical assistance and Yu. G. Kuznetsov, S. B. Larson, M. Plomp, and P. Vekilov for discussions. The National Aeronautics and Space Administration (Grant NAG8-1569) supported this research.

References and Notes

(1) Malkin, A. J.; Kuznetsov, Yu. G.; McPherson, A. *Proteins: Struct. Funct. Genet*. **1996**, *24*, 247.
(2) Rosenberger, F. *J. Cryst. Growth* **1996**, *166*, 40.
(3) Malkin, A. J.; Kuznetsov, Yu. G.; McPherson, A. *J. Struct. Biol.* **1996**, *117*, 124.
(4) Dobrianov, A.; Caylor, C.; Lemay, S. G.; Finkelstein, K. D.; Thorne, R. E. *J. Cryst. Growth* **1999**, *196*, 511.
(5) Yau, S. T.; Petsev, D. N.; Thomas, R. B.; Vekilov, P. G. *J. Mol. Biol*. **2000**, *303*, 667.
(6) McPherson, A.; Malkin, A. J.; Kuznetsov, Yu. G. *Annu. Rev. Biophys. Biomol. Struct.* **2000**, *29*, 361.
(7) Yau, S. T.; Thomas, R. B.; Vekilov, P. G. *Phys. Rev. Lett.* **2000**, *85*, 353.
(8) Galkin, O.; Vekilov, P. G. *Proc. Natl. Acad. Sci. U.S.A.* **2000**, *97*, 6277.
(9) Malkin, A. J.; Kuznetsov, Yu. G.; Lucas, R. W.; McPherson, A. *J. Struct. Biol.* **1999**, *127*, 35.
(10) Chernov, A. A.; Rashkovich, L. N.; Yaminski, I. V.; Gvozdev, N. V. *J. Phys.-Condens. Matter* **1999**, *11*, 9969.
(11) Lomakin, A.; Asherie, N.; Benedek, G. *Proc. Natl. Acad. Sci. U.S.A.* **1999**, *96*, 9465.
(12) Guo, B.; Kao, S.; McDonald, H.; Asanov, A.; Combs, L. L.; Wilson, W. W. *J. Cryst. Growth* **1999,** *196*, 424.
(13) Rosenbaum, D.; Zukoski, C. F. *Phys. Rev. Lett.* **1996**, *76*, 150.
(14) ten Wolde, P. R.; Frenkel, D. *Science* **1997**, *277*, 1975.
(15) Malkin, A. J.; Kuznetsov, Yu. G.; Land, T. A.; DeYoreo, J. J.; McPherson, A. *Nature Struct. Biol.* **1995**, *2*, 956.
(16) Malkin, A. J.; Land, T. A.; Kuznetsov, Yu. G.; McPherson, A.; DeYoreo, J. J. *Phys. Rev. Lett.* **1995**, *75*, 2778.
(17) Wikoff, W. R.; Tsai, C. J.; Wang, G.; Baker, T. S.; Johnson, J. E. *Virology* **1997**, *232*, 91.
(18) Palukaitis, P.; Roossinck M. J.; Dietzgen, R. G.; Francki, R. I. B. *Adv. Virus Res.* **1992**, *41*, 281.
(19) Lot, H.; Marrow, J.; Quiot, J. B.; Esvan, C. *Ann. Phytopathol*. **1972**, *4*, 25.
(20) Bohringer, M.; Jiang, Q.; Berndt.; Schneider, W.-D.; Zegenhagen, J. *Surf. Sci.* **1996**, *367*, 245.
(21) Suzuki, T.; Omori, S.; Nihei, Y. *Surf. Sci.* **1999**, *440*, L881.
(22) Holland, B. T.; Blandford, C. F.; Do, T.; Stein, A. *Chem. Mater*. **1999**, *11*, 795.
(23) Blundell, T. L., & Johnson, L. N. *Protein Crystallography*; Academic Press: New York, 1992.
(24) Helliwell, J. R. *Macromolecular Crystallography with Synchrotron Radiation*; Cambridge University Press: New York, 1992.
(25) Canady, M. A.; Larson, S. B.; Day, J.; McPherson, A. *Nat. Struct. Biol.* **1996**, *3*, 771.
(26) Lucas, R. W.; Kuznetsov, Yu. G.; Larson, S. B.; McPherson, A. *Virology*, in press.
(27) Larson, S. B.; Day, J.; Greenwood, A.; McPherson, A. *J. Mol. Biol.* **1998**, *277*, 37.
(28) Smith, T. J.; Chase, E.; Schmidt, T.; Perry, K. L. *J. Virology* **2000**, *74*, 7578.
(29) Chernov, A. A. *Modern Crystallography III: Crystal Growth*; Springer-Verlag: Berlin, 1984.
(30) Voronkov, V. V. *Sov. Phys. Cryst*. **1970**, *15*, 19.
(31) Kuznetsov, Yu. G.; Konnert, J.; Malkin, A. J.; McPherson, A. *Surf. Sci.* **1999**, *440*, 69.